

Dielectric heating effects of dual-frequency liquid crystals

Chien-Hui Wen and Shin-Tson Wu^{a)}

College of Optics and Photonics, University of Central Florida, Orlando, Florida 32816

(Received 21 March 2005; accepted 2 May 2005; published online 3 June 2005)

A noncontact birefringence probing method is developed to monitor the temperature rise of dual-frequency liquid crystals (DFLCs) due to the dielectric heating effect. This method allows us to determine the temperature change accurately without using a thermocouple. The dielectric heating effects of three DF LC mixtures are investigated quantitatively. By properly choosing the molecular structures, the dielectric heating effect can be minimized while keeping other desirable physical properties uncompromised. © 2005 American Institute of Physics.
[DOI: 10.1063/1.1944889]

Dual-frequency liquid crystals (DFLCs) exhibit a feature that their dielectric anisotropy ($\Delta\epsilon$) changes from positive at low frequencies to negative as the frequency passes the crossover frequency (f_c).¹⁻³ By biasing the DF LC device at a constant voltage while switching the frequency, submillisecond rise and decay times can be achieved.^{4,5} Because of this attractive property, there is a renewed interest in using DF LC for high-speed photonics, such as adaptive optics and diffractive optics.⁶⁻⁹ However, dielectric heating is a big concern for all the DF LC devices. The imaginary part of the dielectric constant of a DF LC absorbs the high-frequency electric field and generates heat, which in turn shifts the crossover frequency.^{1,2,10} As a result, the switching behavior, especially greyscales, of the DF LC drifts.

To quantify the dielectric heating phenomenon, several reports have discussed how the operating voltage affects the sample temperature.^{11,12} Normally, the temperature of the LC cell was monitored by an attached thermocouple. The measured temperature represents the average temperature of the sample cell, not the actual temperature of the LC inside the cell. Beside the experimental characterization method, a more challenging technical issue is how to reduce the dielectric heating effect from molecular engineering standpoint so that the DF LC performance can be better controlled.

In this letter, we develop a noncontact method to measure the transient temperature rise under different voltages and frequencies of the DF LC by probing the birefringence (Δn) decrease. Through these measurements, we are able to quantitatively evaluate the dielectric heating effects.

For a homogeneously aligned DF LC cell, the dielectric heating causes the LC temperature to increase which, in turn, decreases the effective birefringence of the LC layer. The birefringence change can be measured by monitoring the transmittance change of the LC cell sandwiched between two crossed polarizers.¹³ The LC temperature will eventually reach equilibrium between the dielectric heating and the heat dissipation to the air through the substrates. By monitoring the total phase retardation (δ) of the DF LC cell at a laser wavelength (λ), the effective birefringence (Δn) can be calculated from $\delta = 2\pi d\Delta n/\lambda$, where d is the cell gap. Moreover, the LC birefringence decreases with increasing temperature as:¹⁴

$$\Delta n(T) = (\Delta n)_0(1 - T/T_c)^\beta, \quad (1)$$

where $(\Delta n)_0$ is the LC birefringence in the crystalline state (or $T=0$ K), the exponent β is a material constant, and T_c is the clearing temperature of the LC material studied. Therefore, the transient temperature of the DF LC material due to dielectric heating could be measured directly by scanning the transmittance of the LC cell between crossed polarizers.

The dielectric heating-induced temperature rise (ΔT) can be expressed as following:²

$$\Delta T = \left(\frac{V^2 A \epsilon_0 (\epsilon_s - \epsilon_\infty)}{d(C + q_1 t)} \right) \left(\frac{\tau_n \omega^2 t}{(1 + \omega^2 \tau_n^2)} \right), \quad (2)$$

where A is the electrode area, d is the DF LC layer thickness, V is the applied voltage, ϵ_s and ϵ_∞ are the low- (static) and high-frequency dielectric constants of the respective dispersion region, $\tau_n (=1/\omega_n)$ is the relaxation time, t is the dielectric heating time, ω is the angular frequency, C is the average heat capacity of the cell, and q_1 is the specific heat conductivity of the substrates. C is primarily determined by the indium-tin-oxide glass substrates and the LC layer. From Eq. (2), the temperature increase in the LC layer is related to the applied voltage, frequency, duration, electrode area, cell gap, and LC thermal properties. In experiments, we kept the cell gap at $d=8 \mu\text{m}$ and electrode area at $A=0.25 \text{ cm}^2$, and stud-

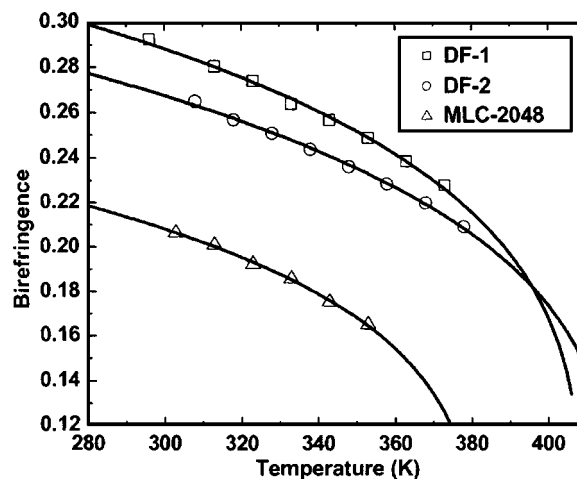


FIG. 1. Temperature-dependent birefringence of DF-1, DF-2, and MLC-2048. Squares, circles, and triangles are measured data for DF-1, DF-2, and MLC-2048, respectively. Solid lines are fitting results using Eq. (1); $\lambda = 633 \text{ nm}$.

^{a)}Electronic mail: swu@mail.ucf.edu

TABLE I. Physical properties of DF-1, DF-2, and MLC-2048. T_m : melting temperature, T_c : clearing point; Δn : birefringence at $\lambda=633$ nm; γ_1/K_{11} : viscoelastic coefficient at $T=23$ °C; and $\Delta\epsilon$: dielectric anisotropy at $f=1$ kHz; f_c : crossover frequency; and E : activation energy.

Mixtures	T_m (°C)	T_c (°C)	Δn	γ_1/K_{11}	$\Delta\epsilon$	f_c (kHz)	E (meV)
DF-1	-48.6	139.3	0.29	21.5	5.7	7.4	514
DF-2	<-50	145.4	0.27	17.8	7.5	10.0	711
MLC-2048	<-50	108.5	0.21	13.8	2.8	23.0	775

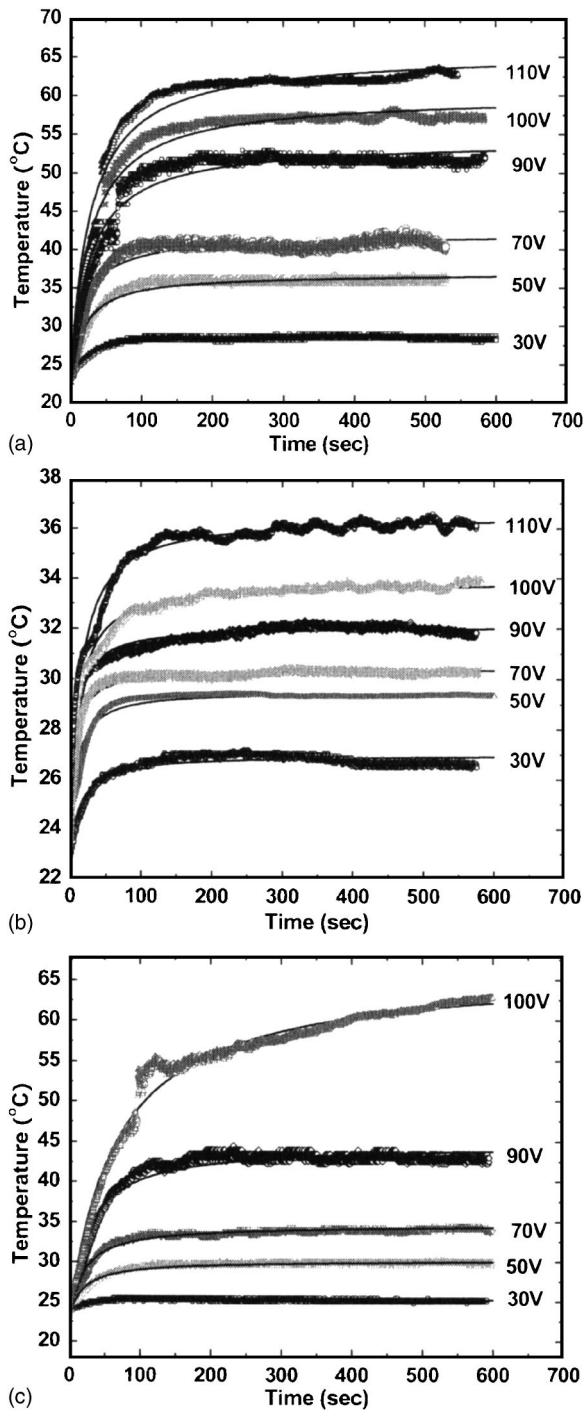


FIG. 2. Measured transient temperature rise of (a) DF-1, (b) DF-2, and (c) MLC-2048 cells at $f=70, 80,$ and 120 kHz, respectively, while varying the applied voltage. The starting temperature is $T=23$ °C. The solid lines are fittings with Eq. (2); the fitting parameters are listed in Table II.

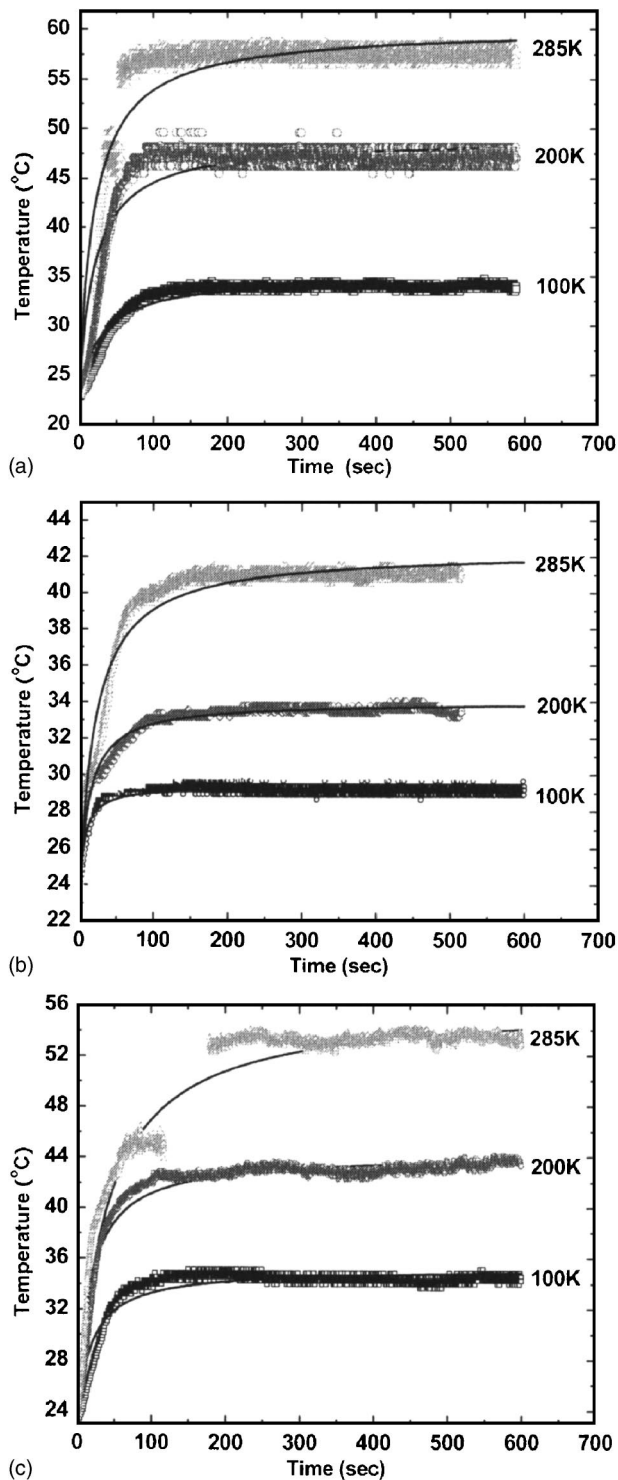


FIG. 3. Measured transient temperature rise of (a) DF-1, (b) DF-2, and (c) MLC-2048 cells at $V=50$ V_{rms} while varying the applied frequency. The starting temperature is $T=23$ °C. The solid lines are fittings with Eq. (2); the fitting parameters are listed in Table III.

ied the voltage and frequency effects on the dielectric heating of the DFLC samples.

To compare the dielectric heating effect of different materials, we formulated two DFLC mixtures, DF-1, DF-2, and compared results with a Merck high Δn DFLC mixture MLC-2048. Our mixtures DF-1 and DF-2 consist of positive $\Delta\epsilon$ biphenyl esters and negative $\Delta\epsilon$ lateral difluoro tolanes at different percentages. Table I lists the key physical properties of these three mixtures.

TABLE II. Parameters obtained by fitting the transient temperature change of DF-1, DF-2, and MLC-2048 using Eq. (2). C is the average heat capacity of the cell and τ_n is the dielectric relaxation time.

$V(V_{\text{rms}})$	DF-1		DF-2		MLC-2048	
	70 kHz		80 kHz		120 kHz	
	$\tau_n(\mu\text{s})$	C	$\tau_n(\mu\text{s})$	C	$\tau_n(\mu\text{s})$	C
30	1.6977	13.54	0.3332	12.82	0.3613	4.43
50	1.1678	18.04	0.2992	6.91	0.3076	16.12
70	0.7026	15.88	0.1702	4.83	0.2498	16.48
90	0.7003	21.99	0.1269	5.85	0.2824	21.41
100	0.6674	22.06	0.1217	8.72	--	--
110	0.6296	24.05	0.1254	11.10	--	--

We first measured the temperature-dependent birefringence of each mixture. Results are plotted in Fig. 1. Dots are the experimental data and solid lines are the fittings by using Eq. (1). These data are used to determine the temperature rise of the DF-LC mixtures during operations. We also measured the frequency-dependent dielectric constants (ϵ_{\parallel} and ϵ_{\perp}) of the three DF-LC mixtures by the capacitance method using a homogeneous cell and a homeotropic cell.^{3,15} The dielectric anisotropy of DF-1, DF-2, and MLC-2048 was measured to be 5.7, 7.5, and 2.8, respectively, at room temperature ($T \sim 23$ °C) and $f = 1$ kHz. A large $\Delta\epsilon$ is favorable because it would lower the operating voltage. The crossover frequency of DF-1, DF-2, and MLC-2048 was measured to be 7.4, 10, and 23 kHz at room temperature. The crossover frequency is dependent on the temperature as: $f_c \sim \exp(-E/kT)$, where k is the Boltzmann constant, and E is the activation energy which is related to the material properties. From the temperature-dependent crossover frequency measurement, the activation energy can be extracted. The activation energy of DF-1, DF-2, and MLC-2048 is 514, 711, and 775 meV, respectively. The smaller activation energy of DF-1 means its crossover frequency is less sensitive to the temperature variation.

To assess the dielectric heating of DF-LC mixtures, we conducted two experiments. First, we drove the LC cells at a fixed frequency but varying the applied voltage. The operating frequency of each DF-LC was chosen when the negative $\Delta\epsilon$ first reaches the saturation value, which is 70, 80, and 120 kHz for DF-1, DF-2, and MLC-2048, respectively. Figures 2(a)–2(c) represent the transient temperature rise of DF-1 (at $f = 70$ kHz), DF-2 (at $f = 80$ kHz), and MLC-2048 (at $f = 120$ kHz), respectively, at various voltages. In the second experiment, we drove the LC cell at $V = 50 V_{\text{rms}}$ but varying the applied frequency. Figures 3(a)–3(c) plot the transient temperature rise of DF-1, DF-2, and MLC-2048, respectively.

In Figs. 2 and 3, the dots represent the experimental data and solid lines represent the fittings with Eq. (2) using $q_1 = 0.8 \text{ W m}^{-1} \text{ K}^{-1}$ and C and τ_n as adjustable parameters. In general, q_1 is weakly dependent on the temperature, but for simplicity we treated it as a constant. The fitting results agree well with the experimental data shown in Figs. 2 and 3. The fitting parameters are listed in Tables II and III. The dielectric relaxation time decreases as the driving voltage or frequency increases, and DF-2 has the largest relaxation frequency among the three mixtures studied.

TABLE III. Parameters obtained by fitting the transient temperature change of DF-1, DF-2, and MLC-2048 using Eq. (2). C is the average heat capacity of the cell and τ_n is the dielectric relaxation time. $V = 50 V_{\text{rms}}$.

$f(\text{kHz})$	DF-1		DF-2		MLC-2048	
	$\tau_n(\mu\text{s})$	C	$\tau_n(\mu\text{s})$	C	$\tau_n(\mu\text{s})$	C
100	0.4230	24.89	0.1849	6.91	0.9854	15.41
200	0.2291	17.06	0.0794	11.87	0.3786	13.60
285	0.1608	16.64	0.0689	18.83	0.3062	25.68

Let us first compare the results of DF-2 and MLC-2048 because their activation energy is similar. By driving the LC cells at $V = 100 V_{\text{rms}}$, the sample temperature of DF-2 ($f = 80$ kHz) and MLC-2048 ($f = 120$ kHz) was raised to 34 and 63 °C, respectively, within 2 min. Moreover, by driving the LC cell at $V = 50 V_{\text{rms}}$ and $f = 100$ kHz, the sample temperature of DF-2 and MLC-2048 was raised quickly to 29 and 34.5 °C, respectively. The higher f_c and smaller $\Delta\epsilon$ of MLC-2048 demand a higher frequency and a higher operating voltage. As a result, MLC-2048 exhibits a more severe dielectric heating than DF-2.

Next, we compare the dielectric heating effect of DF-1 and DF-2. These two mixtures have similar crossover frequency but DF-1 has lower activation energy than DF-2. By driving the LC cells at $V = 100 V_{\text{rms}}$ for 10 min, the sample temperature of DF-1 ($f = 70$ kHz) and DF-2 ($f = 80$ kHz) was raised quickly to 58 and 34 °C, respectively. Under these circumstances, the corresponding crossover frequency of DF-1 and DF-2 was increased from 7.4 to 49.9 kHz and from 10 to 20.9 kHz, respectively. In principle, the crossover frequency of DF-2 is more sensitive to temperature than DF-1 because of its higher activation energy. However, the dielectric heating of DF-2 is much less than DF-1. Consequently, the temperature rise of DF-2 is less significant than DF-1. The compositions of these two mixtures are somewhat different: DF-1 is based on the biphenyl ester compounds, while DF-2 is based on the biphenyl and cyclohexane-phenyl ester compounds. Therefore, it is possible to formulate a dual-frequency LC mixture whose dielectric heating effect is minimized.

¹H. K. Bücher, R. T. Klingbiel, and J. P. VanMeter, Appl. Phys. Lett. **25**, 186 (1974).

²M. Schadt, Mol. Cryst. Liq. Cryst. **66**, 319 (1981).

³I. C. Khoo and S. T. Wu, *Optics and Nonlinear Optics of Liquid Crystals* (World Scientific, Singapore, 1993).

⁴A. B. Golovin, S. V. Shiyonovskii, and O. D. Lavrentovich, Appl. Phys. Lett. **83**, 3864 (2003).

⁵Y. H. Fan, H. Ren, X. Liang, Y. H. Lin, and S. T. Wu, Appl. Phys. Lett. **85**, 2451 (2004).

⁶D. Dayton, S. Brown, J. Gonglewski, and S. Restaino, Appl. Opt. **40**, 2345 (2001).

⁷S. W. Kang, S. Sprunt, and L. C. Chien, Appl. Phys. Lett. **78**, 3782 (2001).

⁸A. K. Kirby and G. D. Love, Opt. Express **12**, 1470 (2004).

⁹P. T. Lin, X. Liang, H. Ren, and S. T. Wu, Appl. Phys. Lett. **85**, 1131 (2004).

¹⁰W. H. de Jeu and Th. W. Lathouwers, Mol. Cryst. Liq. Cryst. **26**, 225 (1973).

¹¹M. Schadt, Mol. Cryst. Liq. Cryst. **89**, 77 (1982).

¹²M. Schadt, Annu. Rev. Mater. Sci. **27**, 305 (1997).

¹³S. T. Wu, U. Efron, and L. D. Hess, Appl. Opt. **23**, 3911 (1984).

¹⁴I. Haller, Prog. Solid State Chem. **10**, 103 (1975).

¹⁵M. G. Clark, E. P. Raynes, R. A. Smith, and R. J. A. Tough, J. Phys. D **13**, 2151 (1980).